Non-Linear Modelling of Three Dimensional Structures Taking Into Account Shear Deformation

Arezki Adjrad, Youcef Bouafia, Mohand Said Kachi, and Hélène Dumontet

***Abstract*—The flexural behavior of reinforced concrete beams is a well-known problem. In the classical studies about this subject, shear strength is neglected or taken into account by simple formula from the linear theory of elasticity, neglecting flexure and shear interaction. For this reason, these classical methods allow to predict only the flexural fracture modes, not the shearing fracture modes.**

We present in this paper an analytical model able to analyze reinforced concrete structures loaded in combined bending, axial load and shear in the frame of non linear elasticity. In this model, the expression adopted for the section's stiffness matrix does not take into account a constant shearing modulus G=f(E) as in linear elasticity, but a variable shearing modulus which is a function of the shear variation using simply formula.

In this part, we present a calculus model of reinforced concrete beams on the three dimensions (3D). This model of computation is then expanded to spatial structures in the second part. A computing method is then developed and applied to the calculus of some reinforced concrete beams. The comparison of the results predicted by the model with several experimental results show that, on the one hand, the model predictions give a good agreement with the experimental behavior in any field of the behavior (after cracking, post cracking, post steel yielding and fracture of the beam).

***Index Terms*—Beams, concrete, modeling, non linear elasticity, shear modulus.**

I. Introduction

The flexural behavior of reinforced concrete beams is a well-known problem: we may refer for instance to references [1]-[6]. In these classical studies about this subject, shear strength is neglected or taken into account by simple formula of the theory of linear elasticity.

We present an analytical model able to analyze reinforced concrete beams loaded in combined bending, axial load and shear, in the frame of non linear elasticity. In this model, the expression adopted for the stiffness matrix [K_s] of the section takes into account a variable shearing modulus, which is a function of the shear variation (and not a constant shearing modulus $G = f(E)$ as in linear elasticity) using a simply formula.

A computer program, based on methods given and detailed in [3], [4], [7], [8], is then developed and in which leads to the following main results: the history of displacements of structural nodal points, the nodal forces (including the reactions of the supports) and the internal effort in a local system of axes.

Manuscript received October 13, 2013; revised December 23, 2013.

The authors are with University "Mouloud Mammeri" of Tizi-Ouzou, 15000, Algeria (e-mail: adjradarezki@yahoo.fr)

II. General Hypothesis

The structure is discretized into beams elements. Elements are decomposed into intermediate sections in order to evaluate the non linear behavior of concrete and reinforcement. The transverse section of the beam is decomposed into concrete layers and longitudinal reinforcement. The deformation of the section follows Bernoulli's principle.

A step-by-step procedure is adopted to simulate the applied monotonic loading at each stage; iterative loops are completed until reaching force balance state during this iterative procedure for equilibrium of external loads.

The following systems of axes are introduced to study the equilibrium of an element: a fixed global system attached to the structure; a local system concerning the initial position of the element; an intrinsic system linked to the deformed position of the element and an intermediate system related to the translation of the local system to the origin of the intrinsic system.

The evaluation of the displacement field of the elements is made by numerical integration of deformations section by section. The deformations of a section are calculated by use of the intrinsic system. It is assumed that deformation and displacements are small. The geometrical non linearity concerning the deformation of the element is neglected as well as the nodal deformation at the junction of several elements. The second order effects due to node displacements are introduced by a non linear transformation of displacements at element ends from the intrinsic system to the intermediate system.

III. Constitutive Model of Materials

A. Compression Behavior of the Concrete

Many mathematical models of concrete are currently used in the analysis of reinforced concrete structures. Among those models, the monotonic curve introduced by Sargin [9] was adopted in this study for its simplicity and computational efficiency. In this model, the stress strain relationship is:

$$\sigma_{bc} = f_{cj}\frac{k_b(\varepsilon_{bc}/\varepsilon_0)-(k_b^{'}-1)(\varepsilon_{bc}/\varepsilon_0)^2}{1+(k_b-2)(\varepsilon_{bc}/\varepsilon_0)-k_b^{'}(\varepsilon_{bc}/\varepsilon_0)^2} \qquad (1)$$

where σ_{bc} is compressive stress, ε_{bc} is compressive strain, f_{cj} is concrete compressive strength, ε_0 is concrete strain corresponding to f_{cj} , $k_b^{'}$ is parameter allow to adjusting the shape of the descending branch of the curve. For

a normal concrete, it generally takes by $k_b^{'} = k_b - 1$, k_b is parameter adjusting the thick ascending limb of the law and is given by the following equation:

$$k_b = \frac{E_c\, \varepsilon_0}{f_{cj}}$$

where E_c is the longitudinal strain modulus of concrete.

B. Idealization of the Tensile Behavior of Concrete

The parameter On the other hand, we assume that concrete is linearly elastic in the tension region. Beyond the tensile strength, the tensile stress decrease with increasing the tensile strain. In this field, we have adopted the monotonic concrete stress-strain curve introduced by Grelat for describe this decreasing branch (see Fig. 1) [1]. Ultimate failure is assumed to take place by cracking when the tensile strains exceed the yielding strain of the reinforcement. In this model monotonic concrete tensile behavior is described by (2).

$$\begin{aligned} \sigma_{ct} &= E_c \varepsilon_{ct} && (\varepsilon_c < \varepsilon_{ct}) \\ \sigma_{ct} &= -f_{tj} \frac{(\varepsilon_{rt} - \varepsilon_{ct})^2}{(\varepsilon_{rt} - \varepsilon_{ct})^2} && (\varepsilon_{ct} < \varepsilon_c < \varepsilon_{rt}) \\ \sigma_{ct} &= 0 && (\varepsilon_c > \varepsilon_{rt}) \end{aligned} \qquad (2)$$

where σ_{ct} is the tensile stress of concrete, ε_c is the tensile strain of concrete, f_{tj} is the tensile strength of concrete, ε_{ct} is the tensile strain corresponding to f_{tj}, ε_{rt} is the ultimate strain of the steel.

C. Reinforcement Constitutive Law

Reinforcing steel is modeled as a linear elastic and plastic paler; the constitutive curves are shown on Fig. 2. Extreme deformations are laid down by regulation Eurocodes is $10^{o}/_{oo}$ [10].

$$\begin{aligned} \sigma_s &= E_a \varepsilon_s && (\varepsilon_s \le \varepsilon_e) \\ \sigma_s &= f_e && (\varepsilon_e < \varepsilon_s \le \varepsilon_u) \\ \sigma_s &= 0 && (\varepsilon_s > \varepsilon_u) \end{aligned} \qquad (3)$$

where σ_s is the steel stress, ε_s is the steel strain, E_a is steel young modulus, f_e is yield stress of steel, ε_e is the yield strain of steel, ε_u is the ultimate strain of steel.

IV. Concrete Shear Modulus

In the classical studies about this subject, shear strength is neglected or taken into account by simply formula of the theory of linear elasticity. Some advanced methods [2], [3], [6], [8], [11]-[17] calculate a variable concrete shear modulus by solving a complex system of equations; namely equilibrium equations, compatibility equations and constitutive laws of the materials One simple empirical equation for the calculation of the post-cracking shear modulus was proposed in [18]. In this study, we distinguish three phases of behaviour (see Fig. 3). Then we propose formulas to calculate the shear modulus of concrete defined by a parametrical study about some experimental results presented by Vecchio and Collins [16]. Shear modulus is calculated by the linear elasticity before concrete cracking and it is functions of reinforcement and concrete after concrete cracking and after plasticization of steel.

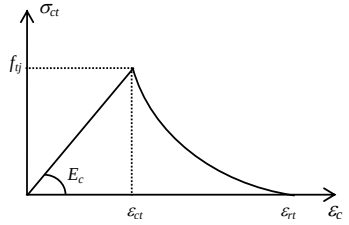

Fig. 1. Model for calculating the tensile behavior of concrete

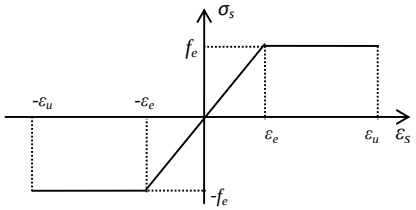

Fig. 2. Idealized stress-strain of the steel

A. Experimental Observations

Fig. 3 shows the curves of shear stress (τ) as a function of shear strain (γ) testing of the walls tested by Vecchio and Collins [16]. The curve comprises a linear phase elastic values $\gamma \le \gamma_{fiss}$ (Phase 1): the transverse deformation modulus (G) is calculated by the linear theory of elasticity. In the second part (phase 2), for values of γ between γ_{fiss} and γ_{plas}, the transverse deformation modulus (G) depends on the characteristics of the concrete and the steel see (6). The phase 3, for values of $\gamma \ge \gamma_{plas}$, corresponds to the plasticization of steels: the modulus G also depends on the characteristics of the materials see (7).

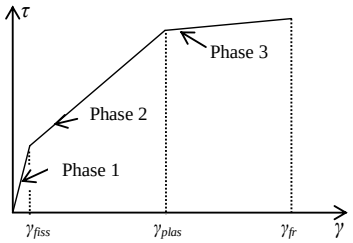

Fig. 3. Shape of the experimental curves (stress-shear strain)

where τ is shear stress, γ is shear strain, γ_{fiss} is the shear strain corresponding to cracking concrete, γ_{plas} is the shear strain corresponding to steel plasticization, γ_{fr} is the shear strain corresponding to cracking of steel.

B. Calculation of Transverse Deformation Modulus G (Proposed Equations)

Phase 1: Before cracking of concrete, the theory of linear elasticity is valid, the transverse deformation modulus G is a function of longitudinal deformation modulus E_c of concrete, and it is given by (5).

Phase 2: After concrete cracking and before plasticization of steel, the transverse deformation modulus G is based on the characteristics of concrete and steel; curve analysis (τ-γ) of experimental tests on walls, tested by Vecchio and Collins

[16] has allowed us to establish a relationship between the transverse deformation modulus G to the characteristics of material see (6) and Table I.

TABLE I: DETAIL OF EXPERIMENTAL AND TESTS AND VERIFICATION OF TRANSVERSE DEFORMATION MODULE G- PHASE 2: AFTER CONCRETE CRACKING AND PHASE 3: AFTER PLASTICIZATION STEELS.

specimen	f_{cj} (MPa)	$\rho_l f_{el}$	$\rho_t f_{et}$	Phase 2: After concrete cracking			Phase 3: After plasticization steels		
				G_{1exp} (MPa)	G_{1calc} (MPa)	G_{1exp}/G_{1calc}	G_{2exp} MPa)	G_{2calc} (Mpa)	G_{2exp}/G_{2calc}
PV1	34,5	8,62	8,11	1020	1224,78	0,83	800	663,09	1,21
PV3	26,6	3,20	3,20	344	232,15	1,48	350	125,68	2,78
PV4	26,6	2,55	2,24	228	148,29	1,54	500	80,28	0,62
PV5	28,3	4,61	4,61	279	453,15	0,62	450	245,33	1,83
PV6	29,8	4,75	4,75	806	456,94	1,76	350	247,38	1,41
PV7	31	8,09	8,09	909	1273,94	0,71	800	689,70	1,16
PV10	14,5	4,93	2,76	682	565,84	1,21	300	306,34	0,98
PV11	15,6	4,19	3,07	568	498,46	1,14	200	269,86	0,74
PV12	16	8,37	1,20	455	379,15	1,20	200	205,27	0,98
PV18	19,5	7,69	1,30	262	309,26	0,85	200	167,43	1,20
PV19	19	8,17	2,13	511	554,05	0,92	200	299,96	0,67
PV20	19,6	8,21	2,63	625	665,08	0,94	250	360,07	0,70
PV21	19,5	8,17	3,91	909	991,10	0,92	300	536,57	0,60
PV22	19,6	8,17	6,40	1140	1612,57	0,71	900	873,03	1,03
PV25	19,2	8,32	8,32	1920	2176,63	0,88	800	1178,41	0,68
PV26	21,3	8,14	4,67	909	1078,28	0,84	504	583,77	0,86
PV27	20,5	7,89	7,89	1360	1834,02	0,74	600	992,92	0,60

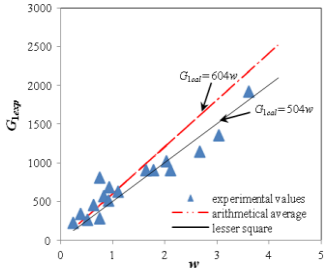

(a) Phase after cracking of the concrete

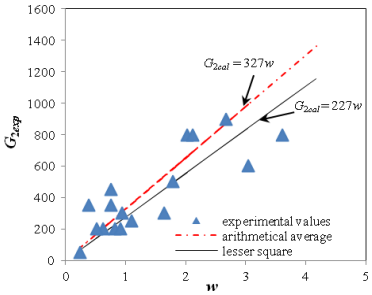

(b) Phase after plasticization of the steels

Fig. 4. Evaluation of the module G from the experimental trials

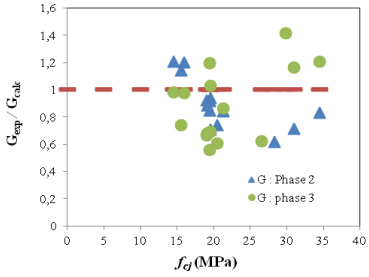

Fig. 5. Comparison of calculated values of G relative to experimental values of G for two phases (2 and 3)

Phase 3: This phase corresponds to the plasticization steels, the transverse deformation modulus G is function as material characteristics see (7) and Table I.

$$\text{We note:} \qquad w = \frac{\rho_t f_{et} \rho_l f_{el}}{f_{cj}} \tag{4}$$

where ρ_t is transverse reinforcement ratio, ρ_l is longitudinal reinforcement ratio, f_{et} is yield stress of transverse reinforcement, f_{el} is yield stress of longitudinal reinforcement, f_{cj} is the concrete compressive strength.

In Fig. 4 we trace *G*, experimental values, depending on the parameter *w*. Of all the tests analyzed, we find that the lines $G = 604w$ and $G = 327w$ include all the experimental points. Therefore, we propose the relationship given in (5), (6) and (7) for the calculation of the transverse module *G*.

$$G = \frac{E_c}{2(1-\mu)} \qquad (0 \le \gamma \le \gamma_{fiss}) \tag{5}$$

$$G = 604w \qquad (\gamma_{fiss} \le \gamma \le \gamma_{plas}) \tag{6}$$

$$G = 327w \qquad (\gamma_{plas} \le \gamma \le \gamma_{fr}) \tag{7}$$

where $\gamma_{fiss} = 0.00003$; $\gamma_{plas} = 0.0025$; $\gamma_{fr} = 0.006$; μ is the Poisson's ratio, it's taken equal 0.2

The Fig. 5 shows the relationship $G_{experimental} / G_{calculus}$ for phases 2 and 3 depending on the compressive strength of concrete.

We give in Tables I the comparison of *G* values calculated

with (6) and (7) and the experimental values for all walls studied.

where G_{1exp} is the shear modulus observed experimentally in the post-cracking stage, G_{2exp} is the shear modulus observed experimentally after plasticization of steels, G_{1calc} is shear modulus calculated using (6), G_{2calc} is shear modulus calculated using (7).

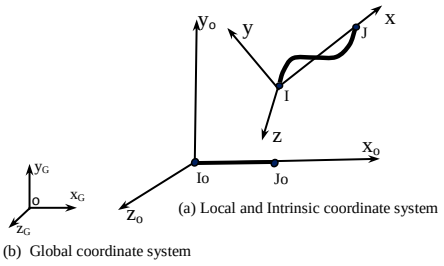

(a) Local and Intrinsic coordinate system

(b) Global coordinate system

Fig. 6. Geometry of the deformed element

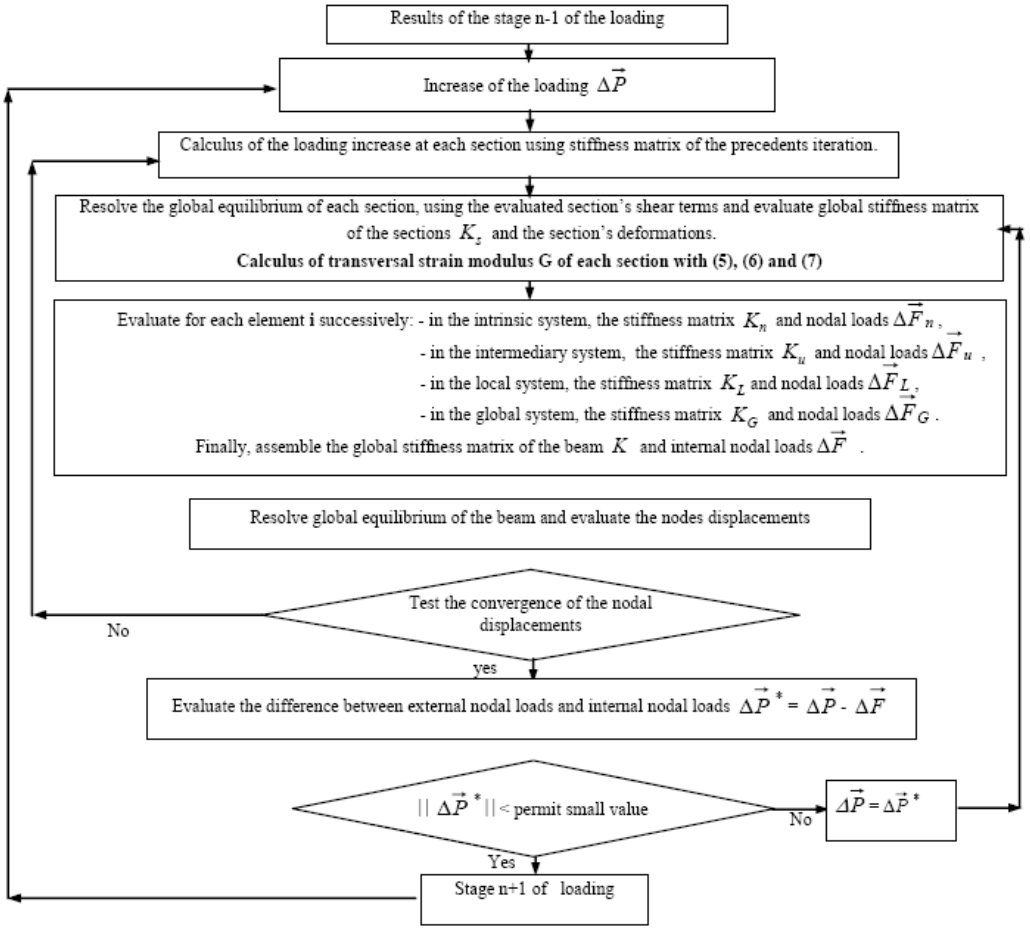

Fig. 7. General organization of the calculus method

V. Procedure for Calculating the Equilibrium State of the Element

The structure is discretized into finite elements. Elements are bars with two nodes and each node has six degrees of freedom: three translations and three rotations.

We consider the global coordinate system $x_G y_G z_G$ and $x_o y_o z_o$ is the local coordinate system related to the initial position of element. Under the effect of loading, I_o node (respectively J_o) of the element is moved I (respectively J). The notion of intrinsic coordinate system, noted xyz axis which connects the first node I to node J is introduced (see Fig. 6).

The notations used in the remainder of this chapter are explained in appendix.

A. Equilibrium of the Section

The equilibrium Equation of the section in the intrinsic system is given by (8); the transversal strain modulus G is calculated using (5), (6) and (7).

$$\Delta\vec{F}_s = K_s\,\Delta\vec{\delta} \tag{8}$$

Equation (8) is solved by an iterative method. Its solution may be written as:

$$\Delta\vec{\delta} = K_s^{-1}\Delta\vec{F}_s \tag{9}$$

B. Calculating the Element Stiffness Matrix in the Intrinsic System

Loads acting over the section are functions of the applied forces at element nodes. Their expression is given by:

$$\Delta\vec{F}_s = L(x)\,\Delta\vec{F}_n \tag{10}$$

If the length variation of the element is neglected, the

expression of the deformation vector $\Delta\vec{S}_n$ of the element, in the intrinsic system, is given using the virtual work theorem which stipulates that the virtual work of the section's deformations increase is equal to the virtual work of the section's loads increase. The expression is shown as:

$$\Delta\vec{S}_n = \int_0^L L^T(x)\,\Delta\vec{\delta}(x)\,dx \tag{11}$$

Thus, we may write the equilibrium equation of the element in the intrinsic system as follows:

$$\Delta\vec{F}_n = K_n\,\Delta\vec{S}_n \tag{12}$$

The stiffness matrix K_n of the element, in the intrinsic system, is evaluated as follows by combining the relationships (9), (10), (11) and (12):

$$K_n^{-1} = \int_0^L L^T(x)\,K_s^{-1}\,L(x)\,dx \tag{13}$$

C. Resolve Global Equilibrium of the Beams Element

The second order effects are introduced by transforming the equation from intrinsic system to intermediate system. In fact, the relationship between the expressions of the displacement in intrinsic and intermediate systems, using a geometrical transformation matrix B , is given by (14).

$$\Delta\vec{S}_n = B\,\Delta\vec{S}_u \tag{14}$$

The equilibrium equation in the intermediate system is given as follows:

$$\Delta\vec{F}_u = (B^T K_n B + D)\,\Delta\vec{S}_u \tag{15}$$

The geometric transformation matrix D is calculated by neglecting the displacement contribution and the non-linear term.

In the local system, using transformation matrix T_0, the element equilibrium may be written as:

$$\Delta\vec{F}_L = T_0^T(B K_n B + D)T_0\,\Delta\vec{S}_L \tag{16}$$

The element stiffness matrix K_L in the local system may finally be written as:

$$K_L = T_0^T(B K_n B + D)T_0 \tag{17}$$

Using the rotation matrix T_G , the equilibrium equation for the global system may be written as:

$$\Delta\vec{F}_G = T_G^T K_L T_G\,\Delta\vec{S}_G = K_G\Delta\vec{S}_G \tag{18}$$

D. Organizational Computing

The procedure described above to determine the equilibrium state of the element is shown in Fig. 7.

VI. Comparison with Experimental Results

A. Tests of Stuttgart (Beams ET)

To validate our approach, we compare the load – deflection curves obtained with the present model and the experimental curves deduced from the shear tests tested by Stuttgart in [19]. These beams have different cross-sections (see Fig. 8) and Table II summarizes the main mechanical characteristics of the materials used.

TABLE II: Material Properties of Stuttgart Tests

Concrete (MPa)	Longitudinal reinforcement (MPa)	transversal reinforcement (MPa)
E_c = 23800	E_a = 210000	E_a = 200000
f_{cj} = 28.5	f_{el} = 420	f_{et} = 320

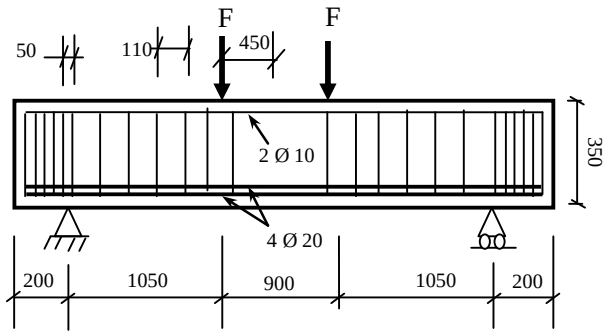

(a) Schematic of loading and detail of reinforcement in beams

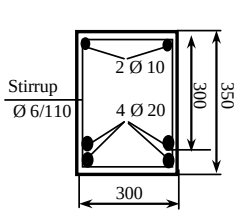

(b) Beam ET1

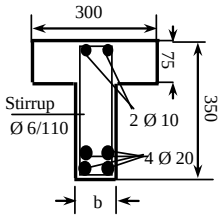

(c) Beam ET2 (b=100 mm)
(d) Beam ET3 (b=150 mm)

Fig. 8. Stuttgart shears test setup, specimen geometry (mm) in [19]

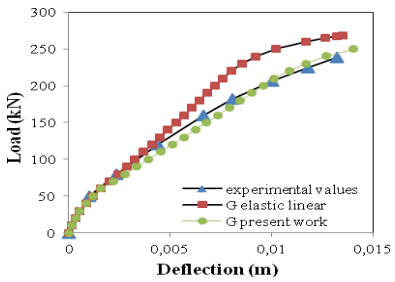

(a) Beam ET1

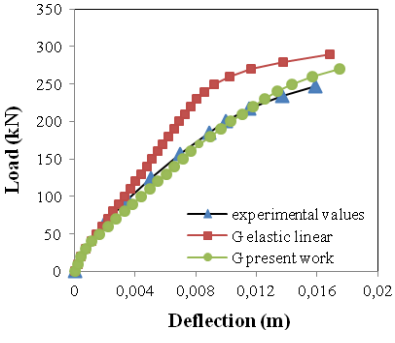

(b) Beam ET2

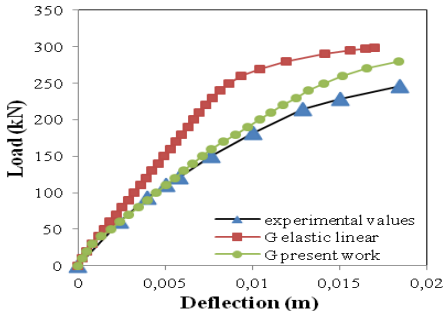

(c) Beam ET3

Fig. 9. Numerical and experimental load-deflection curves for the Stuttgart beams

The superposition of the calculated curves to the experimental curves for the three beams ET1, ET2 and ET3, is given in Fig. 9. The comparison is made on the one hand with respect to the experimental results and also relative to the calculation in the case where G is considered the field of linear elasticity.

It appears that in the case of highly stressed beams in shear, it is essential to take into account the shear deformations in nonlinear to better approximate the experimental curves.

B. *Tests of CEBTP (Beams OG)*

These are two identical beams with respect to the dimensions and reinforcement (see Fig. 10). The beam "OG3" made with normal concrete and the beam "OG4" made with high strength concrete were tested by Four é [20]. The main characteristics of the materials are summered in Table III.

TABLE III: PRINCIPAL CHARACTERISTICS OF THE MATERIALS

Beams	OG3	OG4
Concrete	f_{cj} = 52.5 MPa E_c = 39900 MPa ε_0 = 1.7 f_{tj} = 3.35 MPa	f_{cj} = 71 MPa E_c = 46900 MPa ε_0 = 1.9 f_{tj} = 4.05 MPa
Longitudinal And Transversal Reinforcement	E_a = 205000 MPa f_{el} = 575 MPa f_{et} = 575 MPa	E_a = 210000 MPa f_{el} = 590 MPa f_{et} = 590 MPa

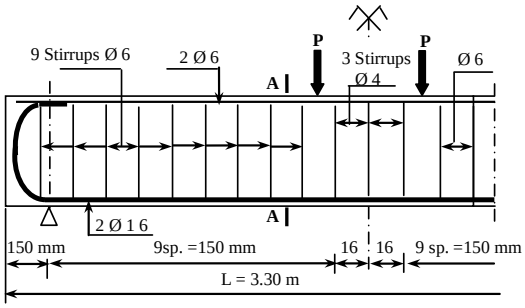

(a) Schematic of test of beams OG

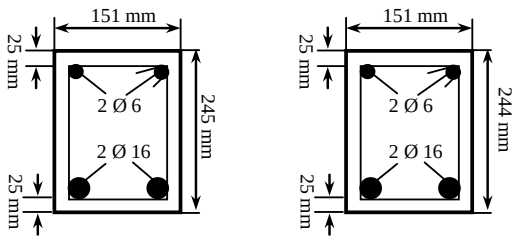

(b) Cross section A-A (OG3) (c) Cross section A-A (OG4)

Fig. 10. Geometry and reinforcement of OG beams; tests of CEBTP [20].

The superposition of the calculated curves to the experimental curves for the two beams OG 3 and OG 4 is given in Fig. 11.

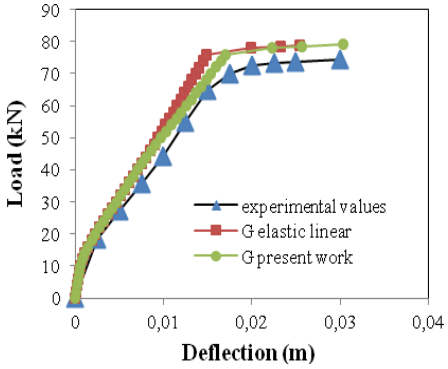

(a) Beam OG3 with the normal concrete

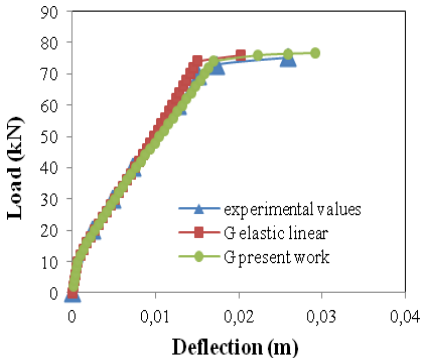

(b) Beam OG4 with the concrete of high strength

Fig. 11. Load-deflection curves for the OG beams

The comparison is made on the one hand with respect to the experimental results and also relative to the calculation in the case where G is considered in the field of linear elasticity.

Curves calculated by taking the current modeling approach better curves obtained experimentally.

C. *Tests of CEBTP (beams HZ)*

The computing method is used for calculation of HZ4 beam tested by Trinh at CEBTP [15]. The dimensions and reinforcement details of the beam are shown on Fig. 12 and the characteristics of the materials are given in Table IV.

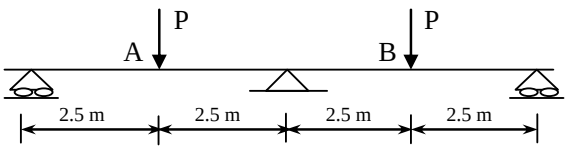

(a) Schematic of loading of the beam HZ4

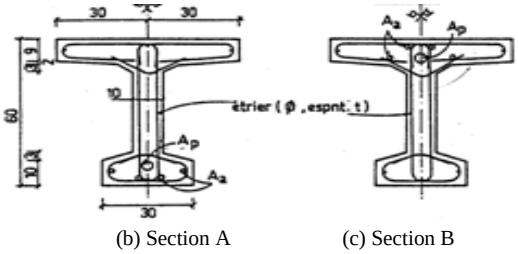

(b) Section A (c) Section B

Fig. 12. Dimensions and details of reinforcement for beam HZ4 tested by Trinh [15].

TABLE IV: STEEL AND CONCRETE CHARACTERISTICS

Concrete				reinforcement			
beam	f_{cj} (MPa)	f_{tj} (MPa)	E_c (MPa)	steel	f_{el} (MPa)	f_{et} (MPa)	E_a (MPa)
HZ4	32	3.3	32000	HA20	424	424	19500
				HA25	450	450	23000

The Fig. 13 shows the evolution of the beam deflection at the loading point as function of the applied load for the HZ4 beam, in the experience, in proposed method and in a non linear calculus with shear stiffness preserve the linear elastic value.

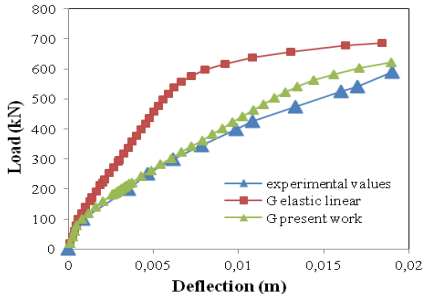

Fig. 13. Load-deflection curves for the beam HZ4

The Fig. 13 clearly shows the importance of taking into account the variation of the shear modulus in the behavior of the beam that the failure occurred by shear.

D. Hyperstatic Continuous Beam (Test of Pera)

The computing method is used for calculation of the beam tested by Pera in [21]. The reinforcement details of the beams are shown on Fig. 14, and the characteristics of the materials are given in Table V.

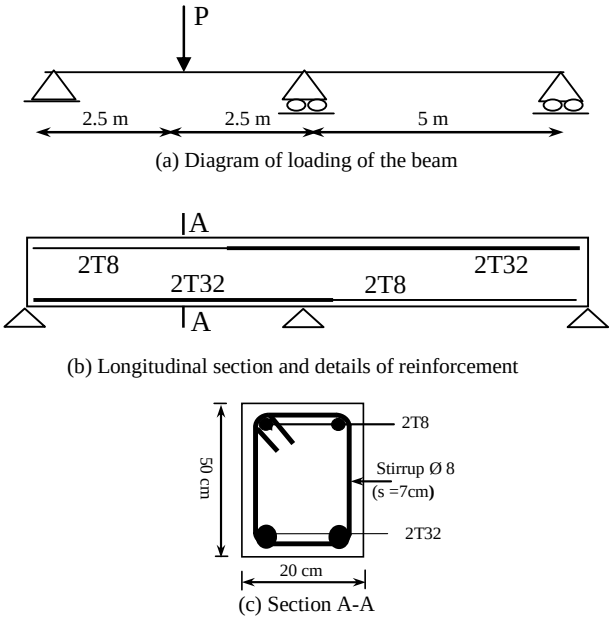

(a) Diagram of loading of the beam

(b) Longitudinal section and details of reinforcement

(c) Section A-A

Fig. 14. Geometrical characteristics and Details of Beam in [21].

TABLE V: MATERIAL PROPERTIES OF PERA TEST

Concrete			Longitudinal and transversal reinforcement		
f_{cj} (MPa)	f_{tj} (MPa)	E_c (MPa)	f_{el} (MPa)	f_{et} (MPa)	E_a (MPa)
41	3.1	25000	368	368	200000

The Fig. 15 shows the evolution of the beam deflection at the loading point as function of the applied load for beam, in the experience, in proposed method and in a non linear calculus with shear stiffness preserve the linear elastic value.

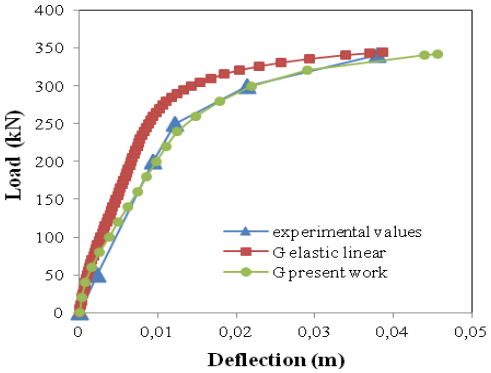

Fig. 15. Load-deflection curves for Pera's beam

The curve calculated with the present study approach very satisfactorily the experimental curve from the point of view of the effort and from the point of view distortion.

E. Cranstan Frame

The computing method is used for calculation of the frame tested by Cranstan in [4]. The reinforcement details of the frame are shown on Fig. 16, and the characteristics of the materials are given in Table IV.

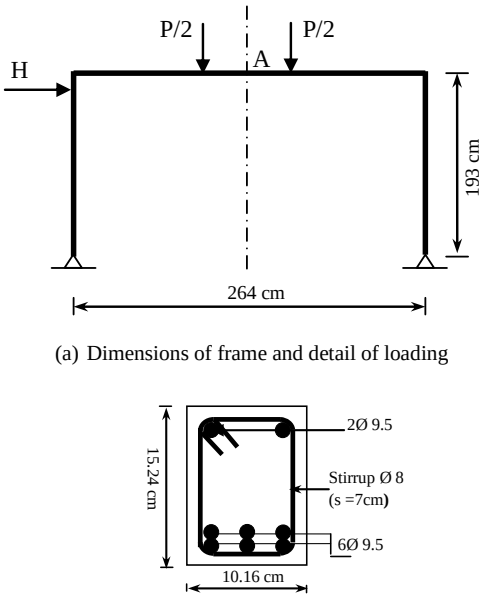

(a) Dimensions of frame and detail of loading

(b) Cross section at mid span

Fig. 16. Geometrical characteristics and details of the reinforcement of the frame tested by Cranstan in [4].

TABLE IV: CHARACTERISTICS OF THE MATERIALS

Concrete	Longitudinal and transversal reinforcement
f_{cj} = 34 MPa	
f_{tj} = 2.59 MPa	f_{el} = 278 MPa
K_b = 1.15	f_{el} = 278 MPa
K'_b = 2.15	E_a = 200000 MPa
ε_0 = 0.0002	
E_c = 34 000 MPa	

The Fig. 17 shows the evolution of the frame deflection at the mid span as function of the applied load for beams, in the experience, in proposed method and in a non linear calculus

with shear stiffness preserve the linear elastic value.

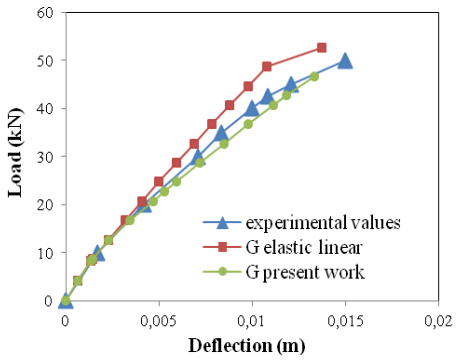

Fig. 17. Load-deflection curves for the Cranstan frame

We can see at the experimental and numerical load-deflection response for this structure exhibit a good agreement for the various stages of the behaviour comparatively to the calculus with shear modulus is constant given by the linear elasticity.

VII. Conclusion

We presented a model based on the strip-analysis of the sections using a simply formula for the shear modulus tanked into a count not constant of the linear elasticity but variable with the variation of the shear strain. This model is able to predict the behaviour of beams with sections having unusual shapes or reinforcing details, loaded in combined bending, axial load and shear.

Indeed, the predicting results of the model compared with the test results show that, on the one hand, the model predictions are in good agreement with the experimental behaviour in any field of the behaviour (after cracking, post cracking, post steel yielding and fracture of beam), and, on the other hand, the model permits to predict shearing fracture modes for reinforced concrete beams (see the beam HZ4, Fig. 13) and flexion fracture mode (see Fig. 15 and 17).

In perspective, it is to introduce this procedure in the case of other types of structures, such as; beams with external prestressing, concrete beams reinforced with metal fibers, tubular sections and beams - reinforced concrete walls

Appendix

The notations used in chapter V, which shows the procedure for calculating the equilibrium of the element, are described below.

K_s is the section stiffness matrix in the intrinsic system.

$\Delta\vec{F}_s$ is vector of exterior loads increase of the cross section it's expression is given by:

$$\Delta\vec{F}_s = \left(\Delta N(x), \Delta M_y(x), \Delta M_z(x), \Delta V_y(x), \Delta V_z(x), \Delta Mc(x)\right)^T$$

Where ΔN is the axial load increase, ΔM_y is the bending moment increase about y axis, ΔM_z is the bending moment increase about z axis, ΔV_y is the shear increase in the y axis, ΔV_z is the shear increase in the z axis, ΔMc is the torsion moment increase.

$\Delta\vec{\delta}$ is increase deformation vector of the section, given by the following equation:

$$\Delta\vec{\delta} = \left(\Delta\varepsilon_g, \Delta\phi_y, \Delta\phi_z, \Delta\gamma_y, \Delta\gamma_z, \Delta\phi_x\right)^T$$

where $\Delta\varepsilon_g$ is the axial strain increase, $\Delta\phi_y$ is the curvature increase about *y*-axis, $\Delta\phi_z$ is the curvature increase about *z*-axis, $\Delta\gamma_y$ is the shear deformation increase about *y*-axis, $\Delta\gamma_z$ is the shear deformation increase about *z*-axis, $\Delta\phi_x$ is the torsional increase about *x*-axis.

$L(x)$ is the matrix connecting the loads acting on the section and the forces applied to the nodes of the element, it is given by:

$$[L(x)] = \begin{bmatrix} -1 & 0 & 0 & 0 & 0 & 0 \\ 0 & \left(1-\frac{x}{\ell}\right) & 0 & 0 & -\frac{x}{\ell} & 0 \\ 0 & 0 & -\left(1-\frac{x}{\ell}\right) & 0 & 0 & \frac{x}{\ell} \\ 0 & 0 & \frac{1}{\ell} & 0 & 0 & \frac{1}{\ell} \\ 0 & -\frac{1}{\ell} & 0 & 0 & -\frac{1}{\ell} & 0 \\ 0 & 0 & 0 & -1 & 0 & 0 \end{bmatrix}$$

where *x* is the abscissa of the cross section relative to intrinsic system coordinates. ℓ is the length of the element after deformation.

$\Delta\vec{F}_n$ is nodal loads increase in the intrinsic system coordinates.

$\Delta\vec{F}_u$ is nodal loads increase in the intermediate system coordinates.

$\Delta\vec{F}_L$ is nodal loads increase in the local system coordinates.

$\Delta\vec{F}_G$ is nodal loads increase in the global system coordinates.

$\Delta\vec{S}_n$ is nodal displacements increase in the intrinsic system coordinates.

$\Delta\vec{S}_u$ is nodal displacements increase in the intermediate system coordinates.

$\Delta\vec{S}_L$ is nodal displacements increase in the local system coordinates.

$\Delta\vec{S}_G$ is nodal displacements increase in the global system coordinates.

K_G is the stiffness matrix of the element in the global system.

References

[1] A. Grelat, "Nonlinear behavior and stability of indeterminate reinforced concrete frames,'' Comportement non Linéaire Et Stabilité Des Ossatures Hyperstatiques En béTon Armé,' Doctoral Thesis, University Paris VI, 1978.

[2] M. S. Kachi, "Modeling the behavior until rupture beams with external prestressing,'' (Modélisation Du Comportement Jusqu' à Rupture Des Poutres À Précontrainte Extérieure), Doctoral Thesis, University of Tizi Ouzou, Algeria, 2006.

[3] M. S. Kachi, B. Fouré, Y. Bouafia, and P. Muller, "Shear force in the modeling of the behavior until rupture beams reinforced and prestressed concrete,'' (l'effort tranchant dans la modélisation du

comportement jusqu'à rupture des poutres en béton armé et précontraint), *European Journal of Engineering*, vol. 10, no. 10, pp. 1235-1264, 2006.
[4] O. N. Rabah, "Numerical simulation of nonlinear behavior of frames Space,'' (Simulation Numérique Du Comportement Non linéAire Des Ossatures Spatiales), Doctoral Thesis, Ecole Centrale de Paris, France, 1990.
[5] F. Robert, "Contribution to the geometric and material nonlinear analysis of space frames in civil engineering, application to structures,'' (Contribution À l'Analyse Non linÉaire Géométrique Et Matérielle Des Ossatures Spatiales En Génie Civil, Application Aux Ouvrages D'art), Doctoral Thesis, National Institute of Applied Sciences of Lyon, France, 1999.
[6] F. J. Vecchio and M. P. Collins, "Predicting the response of reinforced concrete beams subjected to shear using modified compression field theory,'' *ACI Structural Journal*. pp. 258-268, May-June 1988.
[7] A. Adjrad. M. Kachi. Y. Bouafia, and F. Iguetoulène, "Nonlinear modeling structures on 3D,'' in *Proc. 4th Annu.icsaam 2011. Structural Analysis of Advanced Materials*, Romania, pp. 1-9, 2011.
[8] Y. Bouafia, M. S. Kachi, and P. Muller, "Modelling of externally prestressed concrete beams loaded in combined bending, axial load and shear until fracture (in non linear elasticity),'' in *Proc. 2009 ICSAAM. 2009*, Tarbes, France, pp. 1-7, 2009.
[9] M. Virlogeux, "Calculation of non-linear structures in elasticity,'', "Calcul des structures en élasticité non linaire,'' *Annals of Roads and Bridges*, no. 39-40, 1986.
[10] *Calculation of concrete structures Part 1-1: General rules and rules for buildings*, (Calcul des structures en béton, Partie 1-1 : Règles générales et règles pour les bâtiments), Eurocode 2, ENV 1992-1-1, NF P 18 711, 1992.
[11] A. Belarb and T. T. C. Hsu, "Constitutive law of concrete in tension and reinforcing bars stiffened by concrete,'' *ACI Structural Journal*, pp. 465-474, 1994.
[12] A. L. Dall'Asta and R. A Zona, "Simplified method for failure analysis of concrete beams prestressed with external tendons,'' *ASCE Journal of Structural Engineering*, vol. 133, no. 1, pp. 121-131, January 2007.
[13] T. T. C. Hsu, "Non-linear analysis of concrete membrane elements,'' *ACI Structural Journal*, pp. 552-561, 1991.
[14] T. T. C. Hsu and L. X. Zhang, "Tension stiffening in reinforced concrete membrane elements,'' *ACI Structural Journal*, pp. 108-115, 1996.
[15] J. L. Trinh, "Partial prestressing- Tests continuous beams "Précontrainte partielle - Essais de poutres continues,'' *Annals of the Technical Institute of Building and Public Works*, no. 530, pp. 1-31, January 1995.
[16] F. J. Vecchio and M. P. Collins, "The response of reinforced concrete to in-plane shear and normal stresses,'' University of Toronto, Department of Civil Engineering, pp. 82-03, March 1982.
[17] F. J. Vecchio and M. P. Collins, "The modified compression field theory for reinforced concrete elements subjected to shear,'' *ACI Journal*. pp. 219-231, March-April 1986.
[18] K. N. Rahal, "Post-cracking modulus of reinforced concrete membrane elements,'' *Engineering Structures*, vol. 32, pp. 218-255, 2010.
[19] S. Mohr, J. M. Bairan, and A. R. Mari, "A frame element model for the analysis of reinforced concrete structures under shear and bending,'' *Engineering Structures*, vol. 32, pp. 3936-3954, 2010.
[20] B. Fouré, "Deformation limits of tensile reinforcement and concrete in compression for seismic design of structures,'' in *Proc. National Conference AFPS*, Paris, July 2000, vol. II, pp. 67-74.
[21] Z. S. Ameziane, "Cyclic behavior of ordinary concrete and BHP", "Comportement cyclique des bétons ordinaires et des BHP," Doctoral Thesis, Doctoral school, Nantes, France, 1999.

Arezki Adjrad was born on May 6, 1969 in Algeria**.** He has been an assistant lecturer since 2003, at University "Mouloud Mammeri" of Tizi-Ouzou, 15000, Algeria**.** He was also a member of Laboratory LaMoMS (experimental and numerical modeling of materials and structures of civil engineering), UMMTO. He is invested in research themes: materials, experimentation, external prestressing, numerical modeling and nonlinear calculation of structures.

Youcef Bouafia was born on August 29, 1961 in Algeria**.** He has been a professor at University "Mouloud Mammeri" of Tizi-Ouzou, 15000, Algeria since 2003 and he was a lecturer from 1993 to 2003. He was a member of Laboratory LaMoMS (Experimental and Numerical Modeling of Materials and Structures of Civil Engineering), UMMTO**.** He got his PhD from thesis of central School, Paris in 1991. He was director of laboratory "LaMoMS" from 2002 to 2012 and Head of Department of Civil Engineering from 1999 to 2002. Prof. Bouafia is invested in research themes: materials and composites, experimentation, external prestressing, numerical modeling and nonlinear calculation of structures.

Mohand Said Kachi was born on May 3, 1966 in Algeria. He has been a professor since 2012, at University "Mouloud Mammeri" of Tizi-Ouzou, 15000, Algeria and Lecturer from 1993 to 2012. He was a member of Laboratory LaMoMS (Experimental and Numerical Modeling of Materials and Structures of Civil Engineering), UMMTO. He got his PhD from University of Tizi-Ouzou in 2006. He has been a member of the laboratory LaMoMS since 2002. Prof. Kachi is invested in research themes: materials, experimentation, external prestressing, numerical modeling and nonlinear calculation of structures.

Hélène Dumontet is a professor in University of UPMC in France. She is a member of Institu Jean le Rond D'Alembert and works as an associate director of the team MISES modeling and engineering solids. Prof. Dumontet`s research themes are: micromechanics (multi-scale approaches, damage, behavior of materials), fracture mechanics (brittle, ductile, variational approach, and criteria boot Structures (optimization, vibration, stability, nonlinearities, anisotropy).